Infrared emission from the substrate of GaAs-based semiconductor lasers

Mathias Ziegler,[1,a)] Robert Pomraenke,[2] Max Felger,[2] Jens W. Tomm,[1] Parinda Vasa,[2] Christoph Lienau,[2] Marwan Bou Sanayeh,[3] Alvaro Gomez-Iglesias,[3] Martin Reufer,[3] Frank Bugge,[4] and Götz Erbert[4]
[1]*Max-Born-Institut, Max-Born-Str. 2A, 12489 Berlin, Germany*
[2]*Institut für Physik, Carl von Ossietzky Universität, 26111 Oldenburg, Germany*
[3]*OSRAM Opto Semiconductors GmbH, Leibnizstr. 4, 93055 Regensburg, Germany*
[4]*Ferdinand-Braun-Institut für Höchstfrequenztechnik, Gustav-Kirchhoff-Str. 4, 12489 Berlin, Germany*

(Received 10 June 2008; accepted 27 June 2008; published online 28 July 2008)

We report on the origin of three additional low-energy spontaneously emitted bands in GaAs-based broad-area laser diodes. Spectrally and spatially resolved scanning optical microscopy and Fourier-transform infrared spectroscopy assign the different contributions to bandtail-related luminescence from the gain region as well as interband and deep-level-related luminescences from the GaAs substrate. The latter processes are photoexcited due to spontaneous emission from the active region followed by a cascaded photon-recycling process within the substrate.
 [DOI: 10.1063/1.2959854]

The wall-plug efficiency of modern laser diodes is steadily increasing, exceeding 70% for near-infrared (NIR) laser diodes. The remainder is attributed to nonradiative and radiative (spontaneous) recombinations, and leakage currents not used for the laser transition inside the quantum well (QW) gain region.[1,2] In order to get closer to the intrinsic limit and to develop advanced quality assurance techniques, exact knowledge of all the loss mechanisms and their radiative signatures is vital as they directly correspond to degradation/failure modes.[3–9]

In this Letter, we present a study on radiative loss signatures energetically lying between QW transition and blackbody radiation of NIR and red-emitting GaAs-based laser diodes. Application of a Fourier-transform infrared (FTIR) spectrometer and of a near-field scanning optical microscope (NSOM) allows the identification of one signature originating directly from the QW-gain region as well as two additional signatures from the GaAs substrate.

We analyze two completely different epitaxial structures for the red (650 nm) and the NIR spectral range (810 nm). Both high-power broad-area lasers are grown by metal-organic vapor phase epitaxy on a *n*-type GaAs substrate. The red-emitting laser employs an InGaP single QW surrounded by AlGaInP waveguide (WG) and cladding layers, whereas the NIR laser incorporates a GaAsP QW and AlGaAs WG and cladding layers. The stripe widths are 100/130 μm and the resonator lengths 1.2/1.5 mm for the red/NIR devices. More details about the structures can be found in Refs. 10 (red) and 11 (NIR).

Integral emission spectra were recorded with a Bruker IFS 66 FTIR spectrometer equipped with a HgCdTe detector. A homebuilt shear-force-controlled NSOM with spatial resolution of ~200 nm was used for near-field and constant distance emission scans.[12,13] Similar photoluminescence (PL) scans were also performed by exciting the devices by a HeNe laser and collecting the PL signal through the same chemically etched, single mode, and uncoated fiber tip.[12,13] In the emission scans, the fundamental laser wavelengths were filtered out and the laser heat sinks were thermoelectrically stabilized to ambient temperatures. Pulsed-current operation was necessary to avoid overheating of the tip.[14] We recorded 5×5 μm^2 near-field maps with a step size of 0.1 μm and constant distance 60 μm line scans with a step size of 1 μm for both devices. For the near-field scans, the shear-force control was active. For the line scans, the tip was held 4 μm above the sample. We used a deep depletion Si charge coupled device camera for the high-resolution maps of the epilayers and an InGaAs camera for the line scans across the epilayers and half of the substrate.

In Fig. 1 the FTIR emission spectra of the devices are displayed. In spite of the long-wave-pass color filters, residual contributions of the fundamental laser lines at 650 and 810 nm are observed. In red-emitting laser diodes, we observe four major spectral contributions below the laser transition: (i) a shoulder between the filter edge and ~1.7 eV (B1), (ii) a distinct peak around 1.3–1.4 eV (B2), (iii) a very broad (0.7–1.5 eV) band centered of around 1.1 eV (B3), and (iv) the onset of blackbody radiation at ~0.4 eV (B4).

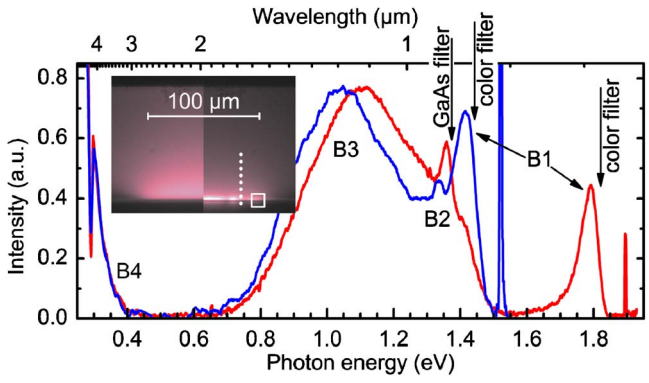

FIG. 1. (Color online) FTIR emission spectra of a red-emitting device (red line) at $I=0.7$ A (heat-sink temperature $T=23$ °C) and a NIR device (blue line) at $I=1.9$ A ($T=50$ °C). The absorption edges of the long-wave-pass color filters at 690 and 850 nm and of GaAs are indicated by arrows. The inset shows micrographs of half the stripe of a *p*-down mounted red-emitting laser diode at $I=0.1$ A (left) and at $I=1.5$ A (right, same region reflected). The scanning regions are marked by a dotted line (line scan) and a square (NSOM map).

a)Electronic mail: mziegler@mbi-berlin.de.

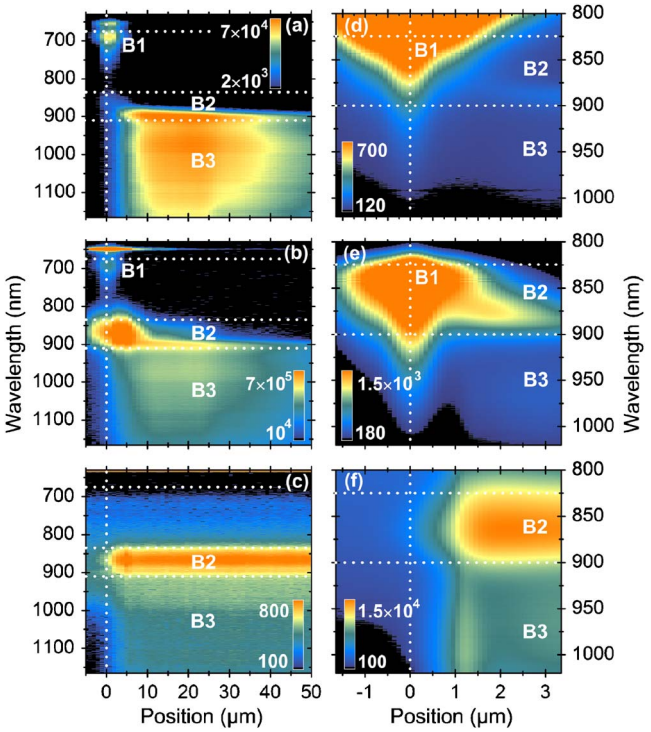

FIG. 2. (Color online) Emission maps of a red-emitting (left panels, step width $\approx 1\ \mu$m) and a NIR (right panels, step width $\approx 0.1\ \mu$m) laser diode at pulsed currents of (a) 0.2 A, (b) 1.0 A, (d) 0.1 A, and (e) 1.0 A and [(c) and (f)] PL maps when excited with a HeNe laser. Filter edges (690 and 825 nm) and emission bands B1–B3 are indicated by dotted horizontal lines. Dotted vertical lines indicate the QW position. The logarithmic scale is chosen to enhance the displayable dynamic range.

For the NIR device, we find the low-energy part of the emission spectrum <1.4 eV very similar to the red-emitting one and the high-energy shoulder B1 shifted to ~ 1.4 eV, following the reduction in lasing energy. Thus, we conclude that B1 is connected to the gain medium, whereas the low-energy emissions (B2,B3) are related to the GaAs substrate as this is common to both laser types. A first proof for this association is given by micrographs (Fig. 1 inset) of the red-emitting device recorded behind a GaAs wafer to suppress stimulated emission and B1 (see GaAs spectral position in Fig. 1). At currents well below threshold (left), the detected emission comes from an extended part of the substrate with its maximum shifted a few microns upwards in position. At higher currents (right) an additional contribution appears that is strongly confined only to a narrow layer of the substrate. Analogous results are obtained from NIR devices.

In order to clarify the association of the low-energy emission (B2,B3) with the substrate, we recorded emission scans at different currents. Selected results after integrating along the epitaxial plane are presented for red-emitting [Figs. 2(a)–2(c)] and NIR [Figs. 2(d)–2(f)] laser diodes. The emission bands initially seen in FTIR are labeled. Additional PL measurements aid in interpretation of the spectra. The WG position (zero in Fig. 2) is found from the fundamental laser-emission maximum, whereas the intense PL signal [Figs. 2(c) and 2(f) at $\lambda \sim 820-900$ nm] starting approximately 1 μm away from the QW marks the position of the GaAs substrate. Thus a clear spatial assignment of the emission B1 with the QW-gain region and of the luminescence (B2,B3) with the GaAs substrate becomes possible. A comparison with the HeNe-laser-excited GaAs PL shows that B2 is the

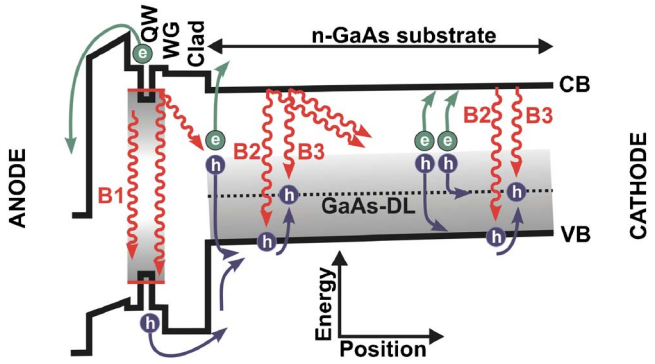

FIG. 3. (Color online) Schematic model picture with CB and VB edges (black lines), DL bands (dotted black lines and gray-shaded regions), QW electron and hole levels (red lines), QW impurity and DL bands (gray-shaded regions), and the radiative transitions B1–B3 (red wavy arrows) of a red-emitting laser diode. The electron (e) and hole (h) leakages are sketched together with the photon-recycling processes.

GaAs interband (IB) luminescence and that a major part of it is reabsorbed in the GaAs substrate for distances of $\gtrsim 2\ \mu$m away from the QW (cf. absorption edge in Fig. 1). A comparison with the micrographs in Fig. 1 shows that B2 may also be guided within the wide-band-gap WG and cladding region.

For the assignment of these emission bands, we use the scheme depicted in Fig. 3. The shoulder B1 represents QW-bandtail emissions caused by various transitions involving localized QW and shallow-impurity and deep-level (DL) states discussed earlier in photocurrent studies.[7,9] The observed bands B2 and B3 are excited within the *n*-GaAs substrate. B2 corresponds to IB transitions,[3] while B3 corresponds to transitions involving radiative recombination centers located below the middle of the GaAs band gap.[8,15] Since the substrate is *n*-type, the IB recombination is governed by the concentration of minority holes, whereas their capture into the DLs results in B3. These transitions can occur due to the reabsorption of spontaneous emission[16] and leakage currents from the active region. In a leakage process, holes are injected into the GaAs substrate after thermionic emission over the cladding layer. The hole-diffusion length within the *n*-substrate is only $\lesssim 1-2\ \mu$m,[17] and the leakage current increases with a rise in temperature.[1,18] We observe, however, decreasing (B2,B3) intensities with increasing heat-sink temperature, ruling out hole-leakage current as the (primary) source of B2 and B3 although reports[1,2] suggests electron leakage into the *p*-cladding to be a significant source of losses in red-emitting lasers.

Reabsorption of fundamental QW-spontaneous emission emitted out of the active layer plane happens inside the GaAs substrate with a penetration depth on the order of 1 μm. As a result, B2 is strongly confined to the cladding/substrate interface. Since B3 is observed over very large distances with its maximum around 20 μm within the substrate, only photonic transport with energies smaller than the GaAs-substrate band gap is left possible and is explained in terms of multiple photon recycling.[19] As depicted in Fig. 3, QW-spontaneous emission (Ref. 16) is transmitted through the wide-band-gap WG/cladding layers and absorbed in a narrow layer of the GaAs substrate adjacent to the cladding. This results in the spontaneous emission of Stokes-shifted B2 and B3 radiation traveling through the substrate. Most of the high-energy part of B2 is subsequently reabsorbed and

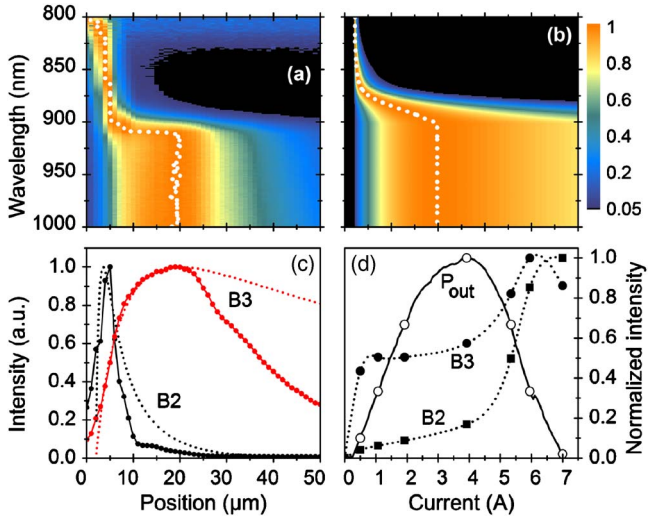

FIG. 4. (Color online) Spatiospectral characteristic of the emission, normalized at every wavelength between 800 and 1000 nm. White dotted lines mark the position of the maxima. (a) Emission map of the red-emitting device at $I=400$ mA; (b) modeled emission intensity fed by reabsorption of the IB-PL starting at 2 μm with $\alpha_{IB}=300\ \mathrm{cm}^{-1}$ including single pass radiation and Fresnel transmission at the GaAs/air interface for n-type GaAs ($N=2\times10^{18}\ \mathrm{cm}^{-3}$); (c) horizontal cuts through (a) as dots with straight lines and (b) as dotted lines, respectively, in black/red for 860–880/950–1000 nm. (d) Emission peaks of around 1.33 eV (B2, full squares) and of around 1.04 eV (B3, full circles), and total front-facet output power (full line) of the NIR device, all normalized vs current at $T=50$ °C.

(partly) reemitted as luminescence B3. The spatial characteristic of this absorption/reemission processes is best visible in Figs. 1 (inset) and 2(b). The normalized emission map of the red-emitting laser is shown in Fig. 4(a). In Fig. 4(b) the photon recycling is modeled as a spatial convolution of the QW excitation and luminescence (B2,B3) partly transmitted at the GaAs/air interface and integrated along the whole cavity length for a single pass through the substrate. The individual contributions are characterized by average energies and exponentially decaying intensities according to an effective absorption coefficient $\alpha(h\nu)$ taken from Ref. 20. Conversely, direct excitation of B3 without involving B2 does not result in a significant lateral shift of the position of the maxima (not shown). Such a cascaded scheme of photon redistribution is specific to laser diodes with emission energies larger than the substrate band edge.

An evidence for the QW-spontaneous emission as the (remote) energy source for the observed long-wavelength luminescence is given from the injection-current dependence of the luminescence peaks in Fig. 4(d). In cw operation, especially at elevated heat-sink temperatures, device heating leads to a decrease in stimulated emission and a concurrent increase in the spontaneous emission strength. Such behavior of B3 is seen in all cases, even for the red-emitting and for long-wavelength, >900 nm, laser devices (not shown), indicating an imperfect spontaneous emission-clamping mechanism. After the rollover, B2 increases more rapidly than B3, indicating different excitation-power dependencies also observed in near-band-edge PL.[21] Furthermore, since the DL concentration is finite, saturation of B3 is expected at a certain injection level as seen in Fig. 4(d).

In conclusion, we found that in GaAs-based laser diodes the QW-spontaneous emission fraction emitted out of the active layer plane photoexcites infrared band-to-band and band-to-DL-defect transitions inside the substrate via a cascaded photon-recycling process. Straightforward noninvasive spectroscopic measurements obtained from the laser front facet provide qualitative information on both the spontaneous emission losses from the gain region and on the defect status of the substrate—even above threshold. We showed that the emergence of the infrared emission from the substrate is not restricted to particular gain materials. Such findings contribute to a better understanding of observed degradation signatures,[3–8] without however providing absolute numbers on their causing losses, and meet the demand for advanced characterization techniques in high-power lasers and laser arrays.

We are indebted to S. Schwirzke-Schaaf and S. Metz for their expert technical and experimental support. We thank I. Esquivias Moscardo and J. M. Garcia Tijero for valuable discussions. Financial support through WWW.BRIGHTER.EU, under Contract No. 035266, and through the German BMBF within the project BRILASI, under Contract No. 13N8601, is gratefully acknowledged.

[1] D. P. Bour, D. W. Treat, R. L. Thornton, R. S. Geels, and D. F. Welch, IEEE J. Quantum Electron. **29**, 1337 (1993).
[2] S. A. Wood, P. M. Smowton, C. H. Molloy, P. Blood, D. J. Somerford, and C. C. Button, Appl. Phys. Lett. **74**, 2540 (1999).
[3] R. L. Hartman and L. A. Koszi, J. Appl. Phys. **49**, 5731 (1978).
[4] U. Imai, K. Isozumi, and M. Takusagawa, Appl. Phys. Lett. **33**, 330 (1978).
[5] D. H. Newman, R. F. Godfrey, A. R. Goodwin, and D. F. Lovelace, Appl. Phys. Lett. **29**, 353 (1976).
[6] M. Ziegler, T. Q. Tien, S. Schwirzke-Schaaf, J. W. Tomm, B. Sumpf, G. Erbert, M. Oudart, and J. Nagle, Appl. Phys. Lett. **90**, 171113 (2007).
[7] T. Q. Tien, F. Weik, J. W. Tomm, B. Sumpf, M. Zorn, U. Zeimer, and G. Erbert, Appl. Phys. Lett. **89**, 181112 (2006).
[8] A. Kozlowska, P. Wawrzyniak, J. W. Tomm, F. Weik, and T. Elsaesser, Appl. Phys. Lett. **87**, 153503 (2005).
[9] C. Ropers, T. Q. Tien, C. Lienau, J. W. Tomm, P. Brick, N. Linder, B. Mayer, M. Müller, S. Tautz, and W. Schmid, Appl. Phys. Lett. **88**, 133513 (2006).
[10] M. Ziegler, J. W. Tomm, T. Elsaesser, C. Matthiesen, M. Bou Sanayeh, and P. Brick, Appl. Phys. Lett. **92**, 103514 (2008).
[11] F. Bugge, A. Knauer, S. Gramlich, I. Rechenberg, G. Beister, J. Sebastian, H. Wenzel, G. Erbert, and M. Weyers, J. Electron. Mater. **29**, 57 (2000).
[12] A. Richter, G. Behme, M. Sueptitz, C. Lienau, T. Elsaesser, M. Ramsteiner, R. Noetzel, and K. Ploog, Phys. Rev. Lett. **79**, 2145 (1997).
[13] C. Lienau, Philos. Trans. R. Soc. London, Ser. A **362**, 861 (2004).
[14] C. Lienau, A. Richter, and T. Elsaesser, Appl. Phys. Lett. **69**, 325 (1996).
[15] J. Pan, J. Mcmanis, M. Gupta, M. Young, and J. Woodall, Appl. Phys. A: Mater. Sci. Process. **90**, 105 (2008).
[16] In addition, a fraction of scattered stimulated emission may act in parallel.
[17] J. H. C. Casey, B. I. Miller, and E. Pinkas, J. Appl. Phys. **44**, 1281 (1973).
[18] C.-M. Wu and E. S. Yang, J. Appl. Phys. **49**, 3114 (1978).
[19] J. L. Bradshaw, W. J. Choyke, R. P. Devaty, and R. L. Messham, J. Appl. Phys. **67**, 1483 (1990).
[20] J. H. C. Casey, D. D. Sell, and K. W. Wecht, J. Appl. Phys. **46**, 250 (1975).
[21] T. Schmidt, K. Lischka, and W. Zulehner, Phys. Rev. B **45**, 8989 (1992).